

Hexatic, Wigner Crystal, and Superfluid Phases of Dipolar Bosons

Kaushik Mitra, C. J. Williams and C. A. R. Sade Melo

Joint Quantum Institute, University of Maryland, College Park, Maryland 20742,
and National Institute of Standards and Technology, Gaithersburg, Maryland 20899

(Dated: February 21, 2024)

The finite temperature phase diagram of two-dimensional dipolar bosons versus dipolar interaction strength is discussed. We identify the stable phases as dipolar superfluid (DSF), dipolar Wigner crystal (DWC), dipolar hexatic fluid (DHF), and dipolar normal fluid (DNF). We also show that other interesting phases like dipolar supersolid (DSS) and dipolar hexatic superfluid (DHSF) are at least metastable, and can potentially be reached by thermal quenching. In particular, for large densities or strong dipolar interactions, we find that the DWC exists at low temperatures, but melts into a DHF at higher temperatures, where translational crystalline order is destroyed but orientational order is preserved. Upon further increase in temperature the DHF phase melts into the DNF, where both orientational and translational lattice order are absent. Lastly, we discuss the static structure factor for some of the stable phases and show that they can be identified via optical Bragg scattering measurements.

PACS numbers: 03.75.Hh, 03.75.Kk, 03.75.Lm

Arguably, one of the next frontiers in ultracold atomic and molecular physics is the study of ultracold heteronuclear molecules such as KRb [1, 2, 3], RbCs [4], and NaCs [5], which can be produced using Feshbach resonances observed in mixtures of two types of alkali atoms [6, 7, 8]. Thus, ultracold heteronuclear molecules consisting of Bose-Bose, Bose-Fermi, or Fermi-Fermi atom pairs offer many new opportunities because of their internal degrees of freedom [9, 10, 11, 12, 13] such as their permanent electric dipole moment.

The dipolar interaction between heteronuclear molecules is highly anisotropic in three dimensions having attractive and repulsive contributions. This makes it generally quite difficult to identify stable phases with good accuracy. In the particular case of bosonic heteronuclear molecules (Bose-Bose or Fermi-Fermi) the attractive part of the dipolar interaction may lead to undesired instabilities of the dipolar gas. However, the situation in two dimensions (2D) can be quite different, and arguably more interesting, as the dipolar interaction can be made to be purely repulsive by the application of suitable static electric or microwave fields. In the case of bosonic dipolar molecules, several stable and metastable many body phases of 2D systems may be found.

In this manuscript, we obtain the finite and zero-temperature phase diagram of bosons interacting via short-range repulsive interactions U and long-ranged dipolar interactions E_D in two-dimensions. For weakly repulsive values of U , and small values of E_D we find a dipolar superfluid phase of the Berezinskii-Kosterlitz-Thouless (BKT) type, which upon increasing values of E_D becomes a dipolar Wigner crystal (DWC) forming a triangular lattice. Numerical evidence for the existence of the DWC phase was obtained recently in Quantum Monte Carlo simulations of dipolar boson systems at zero temperature [14, 15]. Here, however, we develop an analytical variational theory that accounts not only

for the superfluid to DWC phase transition at zero temperature, but also for the finite temperature melting of the DWC into a dipolar hexatic fluid (DHF), where crystalline translational order is destroyed but hexagonal orientational order is preserved. Further temperature increase leads to the melting of the hexatic phase into a dipolar normal fluid (DNF). We also find that the dipolar supersolid phase (DSS), exhibiting both superfluid and crystalline order, has lower (higher) energy than the DSF (DWC) as density or dipole energy increases, but is at least metastable, thus being accessible using thermal quenching. The DSS phase can also melt into a dipolar hexatic superfluid (DHSF). Lastly, we indicate that measurements of optical Bragg scattering can identify the DWC and DHF phases.

Hamiltonian: To describe the phases of interacting dipolar bosons in 2D, we start with the continuum Hamiltonian

$$H = \frac{\hbar^2}{2m} \sum_i \mathbf{r}_i^2 + \frac{1}{2} \sum_{hi,ji} \frac{D}{|\mathbf{r}_i - \mathbf{r}_j|^3} + V_{\text{loc}} \quad (1)$$

where $V_{\text{loc}} = \frac{1}{2} \sum_{hi,ji}^P U(|\mathbf{r}_i - \mathbf{r}_j|)$, and the sum over hi,ji indicate the sum over all pairs of molecules. The first term of H corresponds to the kinetic energy, the second to dipolar interactions, and the third (V_{loc}) to the local (short-range) interaction.

We begin our discussion of different ground states by analyzing first the dipolar Wigner crystal (DWC) phase. In this phase the dipolar interactions are dominant in comparison to the kinetic energy and local energy term s , such that the system crystallizes into a triangular lattice in two dimensions (2D). Thus, our variational wavefunction can be chosen to be

$$\psi_c(\mathbf{r}_1; \mathbf{r}_2; \dots) = \frac{1}{\mathcal{N}} \sum_{p(a)} \prod_i^Y G_{a,i}(|\mathbf{r}_i|) \quad (2)$$

where $\phi_{a_i}(\mathbf{r})$ forms a triangular lattice in 2D, and A is the normalization constant. The $\sum_{\mathbf{P}} \phi_{a_i}(\mathbf{r})$ is a sum over all possible permutations \mathbf{P} of ϕ_{a_i} and the function $G_{a_i}(\mathbf{r}) = \frac{1}{\sqrt{2\pi a^2}} e^{-\frac{(\mathbf{r}-\mathbf{a}_i)^2}{2a^2}}$ is a normalized Gaussian centered at the lattice site \mathbf{a}_i . We define the separation between neighboring lattice sites to be a , and express the boson density as $\rho = \frac{1}{2\pi a^2}$. In addition, we introduce the dimensionless parameters $r_D = \frac{2m}{\hbar^2} D^{-1} = \frac{\hbar^2}{2mU}$ ($r_U = \frac{2m}{\hbar^2} U$) as the ratio of the characteristic dipolar energy $E_D = D^{-3/2}$ (local energy $E_U = U$) and kinetic energy $K = \frac{\hbar^2}{2m}$.

The variational wavefunction described in Eq. (2) is expected to be good for $r_D \gg 1$, where the dipole-dipole interaction is much larger than the kinetic energy, and can be used to compute analytically the average kinetic, local and dipolar energies in terms of the variational parameter $\alpha = \frac{1}{a}$, where a is the Gaussian width and a is the lattice spacing. The dipolar Wigner crystal is only expected for $0 < \alpha < \frac{1}{a_0}$, where its average kinetic energy is $\langle K \rangle_{\text{dwc}} = \frac{N}{3} \frac{\hbar^2}{2m} = \frac{4m}{3} \frac{1}{\alpha^2}$. The average local energy is $\langle V_{\text{loc}} \rangle_{\text{dwc}} = \frac{N}{3} \frac{3U}{\alpha^2} P(\alpha) = \frac{2}{\alpha^2}$ where $P(\alpha) = e^{-1/2\alpha^2} + e^{-3/2\alpha^2} + e^{-2\alpha^2}$ and the average dipolar energy is $\langle V_{\text{dip}} \rangle_{\text{dwc}} = \frac{N}{3} \frac{3KD}{\alpha^2} [P(\alpha) + F(\alpha)] = \frac{2a}{\alpha^2}$ where $F(\alpha) = 1 + 9\alpha^2 + 225\alpha^4 + 8 + 3675\alpha^6 = 16$. In general, $P(\alpha)$ and $F(\alpha)$ are represented by an infinite series in the variational parameter α , but the series is rapidly convergent for $0 < \alpha < 1$, such that the first few terms are sufficient for the discussion of the total average energy $E_{\text{dwc}} = \langle H \rangle_{\text{dwc}}$. The minimization of E_{dwc} with respect to α leads to the minima illustrated in Fig. 1, for $r_U = 0$ and a few values of r_D . For small values of r_D the transition is shifted towards lower values of r_D (not shown in Fig. 1).

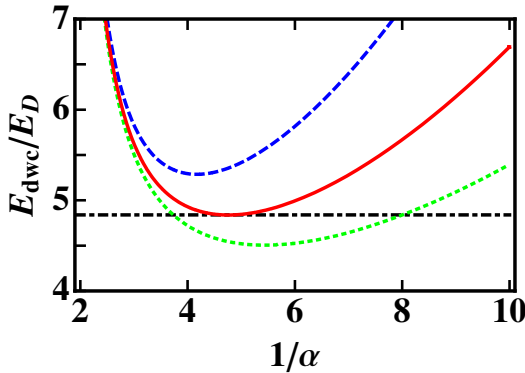


FIG. 1: (Color Online) Plots of the dipolar Wigner crystal energy E_{dwc} in units of the dipolar energy E_D versus the inverse of the variational parameter α for $r_D = 15$ (blue dashed line), $r_D = 26$ (red solid line), $r_D = 47$ (green dotted line). The horizontal black dot-dashed line is the energy E_{dsf} for a uniform superfluid.

Superfluid Phase: The superfluid phase is more easily

described by writing our original Hamiltonian in Eq. (1) in second quantized notation, $H = K + V$, with the kinetic energy $K = \int d\mathbf{r} \frac{\hbar^2}{2m} \nabla^2 \psi^\dagger(\mathbf{r}) \psi(\mathbf{r})$ and potential energy $V = \frac{1}{2} \int d\mathbf{r} d\mathbf{r}' \psi^\dagger(\mathbf{r}) \psi^\dagger(\mathbf{r}') V(\mathbf{r}; \mathbf{r}') \psi(\mathbf{r}) \psi(\mathbf{r}')$; where $V(\mathbf{r}; \mathbf{r}') = D = \frac{\hbar^2}{2m} \frac{1}{r^3} + U(\mathbf{r})$, and $\psi(\mathbf{r})$ is the bosonic field operator which creates a dipolar molecule at position \mathbf{r} . Describing the superfluid phase by the average $\langle \psi^\dagger(\mathbf{r}) \psi(\mathbf{r}) \rangle = \langle \psi^\dagger(\mathbf{r}) \rangle \langle \psi(\mathbf{r}) \rangle = \frac{1}{2}$ leads to the ground state energy $E_{\text{dsf}} = N \left[\frac{3D}{2a} + \frac{U}{2} \right]$; by assuming that the dipolar potential $V_{\text{dip}}(\mathbf{r}) = D = \frac{\hbar^2}{2m} \frac{1}{r^3}$ is unscreened for length scales $r \gg r_0$, and screened to $V_{\text{dip}}(\mathbf{r}) = D = \frac{\hbar^2}{2m} \frac{1}{r_0^3}$ for length scales $r < r_0$, where $r_0 \approx 0.9a$. In Fig. 1, the energy of the DSF phase is shown and compared with that of the DW C phase.

Next, we discuss the melting of the Wigner crystal phase, which occurs in two stages. First the dipolar Wigner crystal melts into a hexatic fluid, which does not have translational order, but preserves rotational order. The melting occurs via the Kosterlitz-Thouless-Nelson-Halperin-Young (KTHNY) dislocation proliferation mechanism. Second, the dipolar hexatic fluid transforms itself into the dipolar normal fluid by losing its rotational order at a higher temperature.

Melting from Wigner Crystal to Hexatic Phase: To study the melting of the DW C phase, we need to calculate its elastic energy. This calculation can be performed by using a semiclassical approximation to the quantum-mechanical method for the calculation of elastic energies [16]. The essential idea is to stretch the many-body wavefunction $\psi(\mathbf{r}_1; \mathbf{r}_2; \dots)$ on each particle coordinate as $\mathbf{r}_i \rightarrow \mathbf{r}_i + \mathbf{u}(\mathbf{r}_i)$ (where repeated indices indicate summation), and expand up to second order in the strain tensor ϵ_{ij} . The resulting elastic energy is

$$E_{\text{el}} = \frac{1}{2} \int d\mathbf{r} \left(2\mu \epsilon_{ij}^2 + \lambda \epsilon_{ii}^2 \right); \quad (3)$$

where $\mu = \frac{15}{32} \frac{\hbar^2}{2m} D = 4a^5$ and $\lambda = 3$ are the unrenormalized Lamé coefficients, and the symmetric (rotation-free) strain tensor is $\epsilon_{ij} = \frac{1}{2} \left(\frac{\partial u_i}{\partial r_j} + \frac{\partial u_j}{\partial r_i} \right)$; with $\mathbf{u}(\mathbf{r})$ being the displacement from equilibrium position.

We follow Ref. [17], and decompose the strain tensor $\epsilon_{ij}(\mathbf{r})$ into a regular (smoothly varying) $\epsilon_{ij}^{\text{reg}}(\mathbf{r})$ and a singular (dislocation) $\epsilon_{ij}^{\text{dis}}(\mathbf{r})$ contribution. Using $k_B = 1$, the Hamiltonian for the smooth part can be written as

$$\frac{H_{\text{reg}}}{T} = \frac{1}{2} \int d\mathbf{r} \left(\frac{2\mu}{a^2} \epsilon_{ij}^{\text{reg}}^2 + \frac{\lambda}{a^2} \epsilon_{ii}^{\text{reg}}^2 \right); \quad (4)$$

where $\mu = \frac{15}{32} \frac{\hbar^2}{2m} D = 4a^5$ and $\lambda = 3$ are the unrenormalized Lamé coefficients, and the symmetric (rotation-free) strain tensor is $\epsilon_{ij} = \frac{1}{2} \left(\frac{\partial u_i}{\partial r_j} + \frac{\partial u_j}{\partial r_i} \right)$; with $\mathbf{u}(\mathbf{r})$ being the displacement from equilibrium position.

$$\frac{H_{\text{dis}}}{T} = \frac{K}{8} \sum_{\mathbf{r} \in \mathbf{r}^0} \mathbf{b}(\mathbf{r}) \cdot \mathbf{b}(\mathbf{r}^0) + \frac{E_c}{T} \sum_{\mathbf{r}} \mathbf{b}(\mathbf{r})^2; \quad (5)$$

where \mathbf{b} is the alpha-component of the Burger's vector \mathbf{b} defined by the contour integral of the displacement

field u around the dislocation: $\nabla^2 u = ab(r)$. Also, the coefficient $K = K_0 a^2 = T$, is related to the unrenormalized Lamé constants through $K_0 = 4(\lambda + \mu) = (2\lambda + \mu)$, and $E_c = (\lambda + 1)KT = 8$ is the core energy associated with a dislocation of core diameter a , while the interaction coefficient is

$$= \ln \frac{[r - r_0]^2}{a} - \frac{[r - r_0]^2}{[r - r_0]^2} \quad (6)$$

To obtain the critical temperature for the melting T_m of the dipolar Wigner crystal we solve the renormalization flow equations for the elastic parameters

$$\begin{aligned} \frac{d}{dl} \frac{1}{\lambda} &= -3Y^2(l)e^{K(l)=8} \\ \frac{d}{dl} (\lambda + \mu) &= -3Y^2(l)e^{K(l)=8} (F_0(l) + F_1(l)); \end{aligned}$$

of the Hamiltonian H_{reg} , where $F_n(l) = I_n(K(l)=8)$, with $I_n(x)$ being the modified Bessel function of order n . These equations need to be solved self-consistently with the flow equations for the parameters

$$\begin{aligned} \frac{dY(l)}{dl} &= -2 \frac{K(l)}{8} Y(l) + 2Y^2(l)e^{K(l)=16} F_0(l) \\ \frac{dK(l)}{dl} &= \frac{3}{2} Y^2(l)e^{K(l)=8} F_0(l) - \frac{3}{4} Y^2(l)e^{K(l)=8} F_1(l); \end{aligned}$$

of the dislocation Hamiltonian H_{dis} . All flow equations are accurate to order Y^3 , where $Y = e^{E_c/T}$ plays the role of the fugacity. The critical temperature T_h is reached when

$$K(T_h) = \frac{4(T_h) - (T_h) + (T_h)}{2(T_h) + (T_h)} = 16 \quad (7)$$

Solving the RG flow equations, we get the melting temperature from the Wigner crystal to the hexatic phase to be $T_h = 0.05E_D$ in the classical limit of $r_D \ll 1$. The melting temperature T_h separating the DWC and DHF phases is shown in Fig. 2.

Transition from Hexatic to Normal Phase: As the dipolar Wigner crystal melts at T_h , translational order disappears but orientational order is preserved, with the emergence of the hexatic order parameter $\phi_6(r) = e^{6i\theta(r)}$. The bond-angle field $\theta(r)$ between the location of the center of masses of the dipolar bosons (heteronuclear molecules) is related to the displacement field $u(r)$ by $\theta(r) = [\partial_x u_y(r) - \partial_y u_x(r)]/2$. The elastic energy for such a situation can be also obtained using a semiclassical approximation to the method of Ref. [16], where each particle coordinate in the many-body wavefunction $(r_1; r_2; \dots)$ is locally rotated $r_i \rightarrow M r_i$, where M is a local rotation matrix (tensor). For the triangular lattice considered here the elastic energy becomes

$$E_{he} = \frac{6}{2} \sum \frac{dr}{a^2} [r - r_0]^2; \quad (8)$$

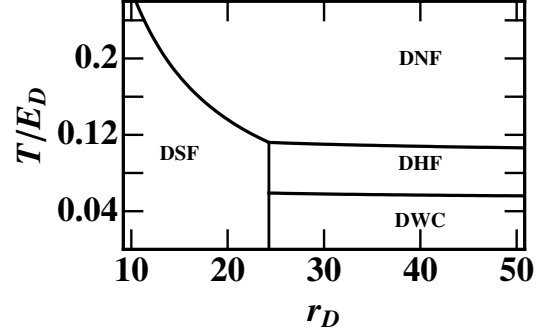


FIG. 2: Finite temperature phase diagram of T/E_D versus r_D showing the dipolar superfluid (DSF), dipolar Wigner crystal (DWC), dipolar hexatic (DHF) and dipolar normal fluid (DNF) phases.

where $\phi_6 = 2E_c$ is the phase stiffness of the hexatic phase, which is directly related to the dislocation core energy $E_c = 1.1KT = 8$. The critical temperature for the disappearance of hexatic order and the emergence of the normal phase T_n is then determined by the RG flow of the 2D-XY model [18], which leads to the condition $\phi_6(T_n) = 72T_n$. The algebraic decay of orientational order is then destroyed at temperature T_n by the dissociation of pairs of ± 3 disclinations, which play the role of vortices and anti-vortices of the standard 2D-XY model. In Fig. 2, the critical temperature T_n separating the phases DHF and DNF is shown as a function of r_D . When $r_D \ll 1$, we obtain $T_n \approx 0.11E_D$ which is larger than the melting temperature of the dipolar Wigner crystal.

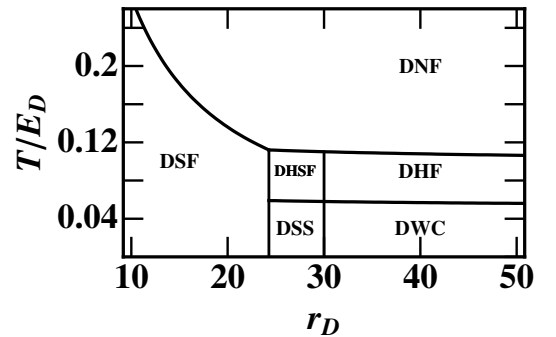


FIG. 3: Phase diagram showing possible dipolar supersolid (DSS) and dipolar hexatic supersolid (DHSF) phases.

Supersolid Phase: Starting from the Hamiltonian defined in the superfluid section we seek a variational solution

$$\psi(r)_{ss} = e_{ss}(r) = \prod_{sf} \frac{1}{\sqrt{2\pi}} + \prod_{ss} \frac{1}{\sqrt{2\pi}} \sum_i G_{a_i; ss}(r); \quad (9)$$

for the supersolid phase, where the Gaussian functions

$G_{\alpha i; \beta ss}(r)$ form a triangular lattice of side a_{ss} . The normalization condition is $\int d\mathbf{r} \rho_{ss}(r)^2 = V$, while $\rho_{ss} = a_{ss}$ is the gaussian width and β is the corresponding variational parameter. The supersolid order parameter $\phi_{ss}(r)$ describes a non-uniform superfluid with both off-diagonal long-range order due to broken $U(1)$ symmetry and diagonal long-range order due to the discrete lattice symmetry. When $\beta \rightarrow \infty$, the energy is essentially that of a superfluid, and when $\beta \rightarrow 0$, the average kinetic energy is $K_{dss} = N \frac{\hbar^2}{3m^2} = (4m^2)$, while the total potential energy is $V_{dss} = V_1 + V_2$, where $V_1 = N \frac{3}{2} U_P(\beta) = (2^2) + N \frac{3}{2} U_D = 8^2$ is the local potential energy and $V_2 = N \frac{3}{2} K_D \left[P(\beta) + F(\beta) \right] = (2a_{ss}) + N \frac{3}{2} D = 4a_{ss}^3$ is the dipolar energy.

We find that the total energy $E_{dss} = K_{dss} + V_{dss}$ of the dipolar supersolid (DSS) phase can be lower than that of the superfluid phase due to the contributions coming from the dipolar interaction, but E_{dss} is always higher than the total energy E_{dwc} of the dipolar Wigner crystal for the same values of parameters. Thus, the transition from the superfluid to the supersolid phase does not occur within our variational ansatz, even if we include additional correlations via Jastrow factors [15]. However, this transition can not be excluded, because only a few classes of variational wavefunctions have been explored. Additionally, we find that the supersolid phase is at least metastable, since E_{ss} has a minimum that can be reached upon thermal quenching, and possibly also melted into a metastable dipolar hexatic superfluid (DHSF). A phase diagram showing possible DSS and DHSF phases is presented in Fig. 3.

Experimental characterization of the various phases: The various phases proposed here can be characterized by the measurement of their density-density correlations, as reflected in the structure factor $S(q) = \ln(q)n(q)/i$, where $n(q)$ is the Fourier transform of the density operator $n(r)$, and the symbol $h::i$ corresponds to both quantum mechanical and thermal averaging.

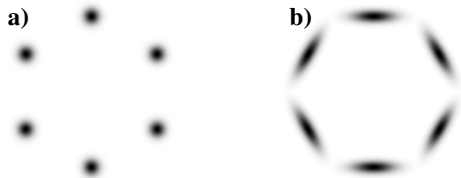


FIG. 4: Bragg scattering patterns near the first reciprocal vectors for a) the dipolar Wigner crystal phase and for b) the dipolar hexatic superfluid phase.

The most dramatic effects in the structure factor are found in dipolar Wigner crystal phase where $S(q) \propto q^{-2+ (G;T)}$ revealing the power law behavior characteristic of two dimensions in the vicinity of the reciprocal lattice (Bragg) vectors G . The first Bragg vector

has magnitude $|G_1| = 4/\sqrt{3}a$, and the Bragg scattering pattern then exhibits 6-fold symmetry below the melting temperature T_m as shown in Fig. 4a. The exponent $(G;T) = (|G_1|/4)(T=)(3+)= (2+)$ is related to the renormalized Lamé coefficients α and β . This reflects the power law decay of the correlation function $C(G;R) \propto R^{- (G;T)}$, which is the Fourier transform of $S(q)$. The profile of $S(q)$ for the dipolar hexatic phase corresponding to a melted dipolar Wigner crystal with orientational order is characterized by the hexagonal pattern shown in Fig. 4b.

Conclusions: We have described some of the possible phases of dipolar bosons in two dimensions, including superfluid, supersolid, hexatic superfluid, Wigner crystal, hexatic and normal fluids. Within our variational approach we have concluded that the supersolid and hexatic superfluid phases may have lower free energy than the superfluid phase in some region of the phase diagram, but do not seem to have lower free energy than the Wigner crystal or hexatic fluid in the same region. However, the supersolid and hexatic superfluid phases are at least metastable, and thus may be reached via thermal quenching, and probed via Bragg scattering. Furthermore, we have shown that dipolar Wigner crystal does not melt directly into a normal fluid, but presents a two-stage melting: first into a hexatic phase which preserves orientational order, and then into a normal fluid upon further increase in temperature. Finally, we indicated the experimental signatures of stable phases with translational or orientational order in a Bragg spectroscopy measurement that detect the static structure factor.

-
- [1] M. W. M. Anciniet al, Phys. Rev. Lett. 92, 13203 (2004).
 - [2] D. Wang et al, Phys. Rev. Lett. 93, 243005 (2004).
 - [3] C. O. Spielkaus et al, Phys. Rev. Lett. 97, 120402 (2006).
 - [4] A. J. Kem et al, Phys. Rev. Lett. 92, 153001 (2004).
 - [5] C. Haimberger et al, Phys. Rev. A 70, 021402(R) (2004).
 - [6] C. A. Stan et al, Phys. Rev. Lett. 93, 143001 (2004).
 - [7] S. Inouye et al, Phys. Rev. Lett. 93, 183201 (2004).
 - [8] F. Ferlaino et al, Phys. Rev. A 73, 040702(R) (2006).
 - [9] K. Goral et al, Phys. Rev. A 61, 051601 (2000).
 - [10] L. Santos et al, Phys. Rev. Lett. 85, 1791 (2000).
 - [11] M. A. Baranov et al, Phys. Rev. A 66, 013606 (2002).
 - [12] T. Rieger et al, Phys. Rev. Lett. 95, 173002 (2005).
 - [13] M. Iskin, C. A. R. Sa de Melo, Phys. Rev. Lett. 99, 11402 (2007).
 - [14] H. P. Buchler et al, Phys. Rev. Lett. 98, 060404 (2007).
 - [15] G. E. Astrakharchik et al, Phys. Rev. Lett. 98, 060405 (2007).
 - [16] O. H. Nielsen, and R. M. Martin, Phys. Rev. B 32, 3780 (1985).
 - [17] David R. Nelson and B. L. Halperin, Phys. Rev. B 19, 2457 (1979).
 - [18] J. M. Kosterlitz, J. Phys. C 7, 1046 (1974).